β-Secretase Cleavage of Alzheimer's Amyloid Precursor Protein by the Transmembrane Aspartic Protease BACE

Robert Vassar *et al.*

Science **286**, 735 (1999);
DOI: 10.1126/science.286.5440.735

Science (print ISSN 0036-8075; online ISSN 1095-9203) is published weekly, except the last week in December, by the American Association for the Advancement of Science, 1200 New York Avenue NW, Washington, DC 20005.

β-Secretase Cleavage of Alzheimer's Amyloid Precursor Protein by the Transmembrane Aspartic Protease BACE

Robert Vassar,[1]* Brian D. Bennett,[1]* Safura Babu-Khan,[1] Steve Kahn,[1] Elizabeth A. Mendiaz,[1] Paul Denis,[1] David B. Teplow,[2] Sandra Ross,[1] Patricia Amarante,[1] Richard Loeloff,[1] Yi Luo,[1] Seth Fisher,[1] Janis Fuller,[1] Steven Edenson,[1] Jackson Lile,[1] Mark A. Jarosinski,[1] Anja Leona Biere,[1] Eileen Curran,[1] Teresa Burgess,[1] Jean-Claude Louis,[1] Frank Collins,[1] James Treanor,[1] Gary Rogers,[1] Martin Citron[1]†

Cerebral deposition of amyloid β peptide (Aβ) is an early and critical feature of Alzheimer's disease. Aβ generation depends on proteolytic cleavage of the amyloid precursor protein (APP) by two unknown proteases: β-secretase and γ-secretase. These proteases are prime therapeutic targets. A transmembrane aspartic protease with all the known characteristics of β-secretase was cloned and characterized. Overexpression of this protease, termed BACE (for beta-site APP-cleaving enzyme) increased the amount of β-secretase cleavage products, and these were cleaved exactly and only at known β-secretase positions. Antisense inhibition of endogenous BACE messenger RNA decreased the amount of β-secretase cleavage products, and purified BACE protein cleaved APP-derived substrates with the same sequence specificity as β-secretase. Finally, the expression pattern and subcellular localization of BACE were consistent with that expected for β-secretase. Future development of BACE inhibitors may prove beneficial for the treatment of Alzheimer's disease.

Alzheimer's disease is characterized by the progressive formation in the brain of insoluble amyloid plaques and vascular deposits consisting of the 4-kD amyloid β-peptide (Aβ) (*1*). Aβ occurs in two predominant forms with different COOH-termini, Aβ40 and Aβ42, and overproduction of Aβ42 has been suggested to be the cause of familial early-onset Alzheimer's disease (*2*). Formation of Aβ requires proteolytic cleavage of a large type-1 transmembrane protein, the β-amyloid precursor protein (APP) (*3*), which is constitutively expressed in many cell types. To initiate Aβ formation, β-secretase cleaves APP at the NH_2-terminus of Aβ to release APPsβ, a ~100-kD soluble NH_2-terminal fragment, and C99, a 12-kD COOH-terminal fragment which remains membrane bound (Fig. 1). In an alternate pathway, α-secretase cleaves within the Aβ sequence, thus precluding the formation of Aβ. Cleavage by α-secretase produces a large soluble NH_2-terminal fragment, APPsα, and a 10-kD membrane-bound COOH-terminal fragment, C83 (Fig. 1). Both C99 and C83 can be further cleaved by one or more γ-secretases, leading to the release and secretion of Aβ and the nonpathogenic p3 peptide, respectively.

Intense efforts have been directed toward the identification of α-, β-, and γ-secretases. Two metalloproteases, ADAM 10 and TACE, are involved in α-cleavage of APP (*4*). Various β-secretase candidates have been described [for review, see (*5*)]. Although most of these candidates can cleave small peptides around the β-secretase site, none have all the predicted characteristics of the enzyme. Activity of γ-secretase has recently been shown to require presenilin (*6, 7*), and on this basis it has been proposed that presenilin 1 is γ-secretase; however, to date there is no evidence that presenilin 1 has proteolytic activity (*7*).

Cell culture studies have defined the functional properties of β-secretase. Most cell types generate Aβ (*8*), indicating that β-secretase is widely expressed. The β-secretase pathway appears more prominent in primary mixed brain cultures than in peripheral cells (*9*), and neurons show more β-secretase activity than astrocytes (*10*). Cell biological studies suggest three potential sites of intracellular β-secretase activity: endosomal/lysosomal compartments, see for example (*11*), Golgi-derived vesicles (*12*), and endoplasmic reticulum/intermediate compartments in postmitotic neurons (*13*). β-secretase has an acidic pH optimum (*14, 15*).

The exact sites of β-secretase cleavage have been determined. Amyloid plaque Aβ starts at Asp1 (*16*), and this cleavage site is therefore of major interest. In human embryonic kidney cells, the majority of Aβ starts at Asp1, but a minority of peptides start at Val-3 and Glu11 (*8*). In contrast, the predominant Aβ species in rat primary neuronal cultures starts at Glu11 (*17*). This NH_2-terminal heterogeneity of Aβ has raised the question of whether one or multiple β-secretase enzymes exist. Inhibitor studies suggest that production of Glu11 peptides parallels that of Asp1 peptides (*17*), whereas Val-3 peptides seem to be generated by a different protease (*18, 19*). β-secretase cleavage is highly sequence-specific. A Met → Leu substitution at the P1 position of APP, found in the "Swedish" familial AD mutation (Fig. 1) which causes early-onset Alzheimer's disease (*20*), dramatically enhances β-secretase cleavage (*21*), but many other substitutions (for example, Met → Val) decrease it (*22*).

We now report the cloning of a human transmembrane aspartic protease, BACE, that has all the known characteristics of the β-secretase.

Identification of the β-secretase candidate BACE. We used an expression cloning strategy to identify genes that modulate Aβ production. APP processing has been extensively characterized in human embryonic kidney 293 cells, and it is well established that these cells express the β- and γ-secretases involved in Aβ production. We constructed a directional cDNA expression library from this cell line in a cytomegalovirus promoter-based expression vector. We transiently transfected ~8600 pools of 100 into a 293 cell line, which overexpresses APP containing the Swedish mutation (APPsw) (*23*). Changes in Aβ levels in conditioned media were monitored by ELISA assays that detect $Aβ_{1-x}$ (total Aβ) and $Aβ_{x-42}$ (Aβ derivatives ending at amino acid 42). Pools that produced elevations in secreted $Aβ_{1-x}$ or $Aβ_{x-42}$ relative to the plate average were selected as positives and subsequently subdivided to single cDNA clones. Of the cDNA pools we identified as positive in the primary screen, one contained a clone that shared significant sequence similarity with members of the pepsin subfamily of aspartic proteases. This clone encodes a novel protein, which we have termed BACE (for beta-site APP cleaving enzyme).

The sequence of the 2526–base pair BACE cDNA revealed an open reading frame of 501 amino acids. The BACE protein has an NH_2-terminal signal peptide of 21 amino acids followed by a proprotein domain spanning amino acids 22 to 45 (*24*). The lumenal domain of the

[1]Amgen, Inc., One Amgen Center Drive, M/S 29-2-B, Thousand Oaks, CA 91320–1799, USA. [2]Department of Neurology, Harvard Medical School, and Center for Neurologic Diseases, Brigham and Women's Hospital, Boston, MA, 02115, USA.

*These authors contributed equally to this work.
†To whom correspondence should be addressed. E-mail: mcitron@amgen.com

mature protein extends from residues 46 to 460, and is followed by one predicted transmembrane domain of 17 residues and a short cytosolic COOH-terminal tail of 24 amino acids.

BACE contains two active site motifs at amino acids 93 to 96 and 289 to 292 in the lumenal domain. Each motif contains the highly conserved signature sequence of aspartic proteases, D $^{T}/_{S}$ G $^{T}/_{S}$, within which the aspartic acid residue is essential for catalytic activity [for review, see (*25*)]. BACE also has four putative N-linked glycosylation sites and six lumenal cysteines, which would allow the formation of up to three intramolecular disulfide bonds (Figs. 1 and 2). Thus, BACE is predicted to be a type I transmembrane protein with the active site on the lumenal side of the membrane, where β-secretase cleaves APP (Fig. 1).

At the amino acid level, BACE shows less than 30% sequence identity with human pepsin family members, with most similarity to cathepsin E (30% identity, 37% similarity). The homology to other pepsins is highest in the central portion of BACE, while the NH_2- and COOH-termini are more divergent. The low sequence similarity of BACE to pepsins together with the putative transmembrane domain indicate that BACE may define a new subclass of membrane-bound aspartic proteases.

Rat and mouse orthologs of BACE were identified in a computer search of an Amgen expressed sequence tag database. The rat (GenBank accession AF190727) and mouse (GenBank accession AF190726) BACE cDNAs have, respectively, 91 and 93% sequence identity, with full-length human BACE cDNA. Both rat and mouse cDNAs encode proteins of 501 amino acids that have 96% sequence identity with the human BACE protein.

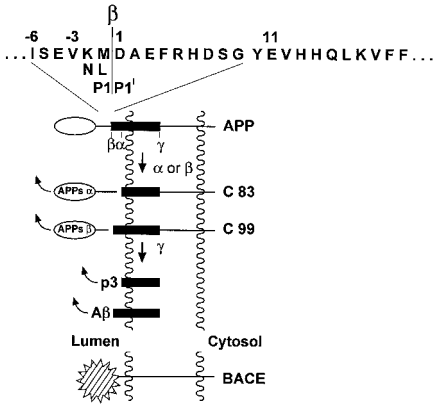

Fig. 1. Schematic structure of APP and BACE (not drawn to scale), showing proteolytic processing sites and cleavage products of APP. Wavy lines represent the cell membrane. The amino acid sequence of APP around the β-secretase cleavage site is numbered relative to the Asp1 start of Aβ. The position of the Swedish APP mutation, a substitution of P2: Lys → Asn and P1: Met → Leu, is indicated.

BACE mRNA expression in peripheral tissues and brain. Most, if not all, cells and tissues express APP and generate Aβ. Therefore, β-secretase expression is expected to have a broad tissue distribution. Northern blot analysis of human BACE mRNA in adult peripheral tissues and various subregions of the brain revealed three transcripts of ~7.0, 4.4, and 2.6 kb (Fig. 3, A and B). With the exception of the pancreas, which exhibits robust expression, most peripheral tissues express low levels of BACE mRNA. Expression in brain and brain subregions is moderately higher with uniform expression observed across all subregions.

To determine which cell types express BACE mRNA in the adult brain, we analyzed adult rat brain sections by in situ hybridization (*26*). At low magnification, the hybridization signal is observed throughout all regions of the adult rat brain, with the strongest signal over hippocampus, cortex, and cerebellum (Fig. 3D). At higher magnification, the signal is observed over most neurons, whereas glia appear to express little or no BACE mRNA (Fig. 3, E and F). Overall, the pattern of BACE mRNA expression is consistent with that expected for the β-secretase.

BACE protein in cells and human brain. To detect the BACE protein, we generated a rabbit polyclonal antiserum directed against the cytosolic COOH-terminal tail corresponding to amino acids 485 to 501. This antiserum was used to immunoprecipitate BACE from normal human brain, AD brain, and 293 cells transfected with BACE cDNA (Fig. 3C). Immunoprecipitates were subsequently analyzed on immunoblots developed with the anti-BACE antiserum (*27*). A protein of ~70 kD is apparent in the transfected 293 cell extract immunoprecipitated with anti-BACE (S) but not in the preimmune immunoprecipitate (0) or when the antiserum is preabsorbed (A) (Fig. 3C). The increased size of the protein observed on immunoblots compared to the predicted size of the mature enzyme (51 kD) is due to N-linked glycosylation, as was determined by analysis of immunoprecipitates incubated with N-glycosidase F (*24*). The ~28-kD immunoprecipitated protein in the 293 cells may represent a degradation product of BACE. Both AD and age-matched control brain homogenates show the ~70-kD protein, which reacts with anti-BACE and comigrates with the transfected BACE (Fig. 3C).

Intracellular localization of BACE. β-secretase activity is highest in compartments of the secretory pathway including the Golgi apparatus, trans-Golgi network (TGN), secretory vesicles, and endosomes. To determine the intracellular localization of BACE protein, we generated a tagged form of BACE with the hemagglutinin (HA) epitope fused to the COOH-terminus of the cytosolic tail (BACE-HA) (*28*). The BACE-HA protein was stably transfected into 293 cells, and the cells were then costained with anti-HA antibodies and antibodies against organelle markers (*29*). A substantial proportion of BACE-HA immunostaining appears in the Golgi and endosomes (Fig. 4A). Similar results were obtained by co-localizing BACE-HA with several other Golgi and endosome markers (β-coatomer protein, furin, Golgi complex antibody-1, early endosome antigen 1), whereas only a small amount of staining is observed in ER and lysosomes (*24*).

The soluble APPsβ fragment (Fig. 1) is a direct product of β-secretase cleavage of APP and therefore is a marker of β-secretase activity. To address whether overexpression of BACE induces β-secretase cleavage within cells, we transiently transfected the BACE-HA stable cell line with APP containing the Swedish mutation (APPsw). Immunocyto-

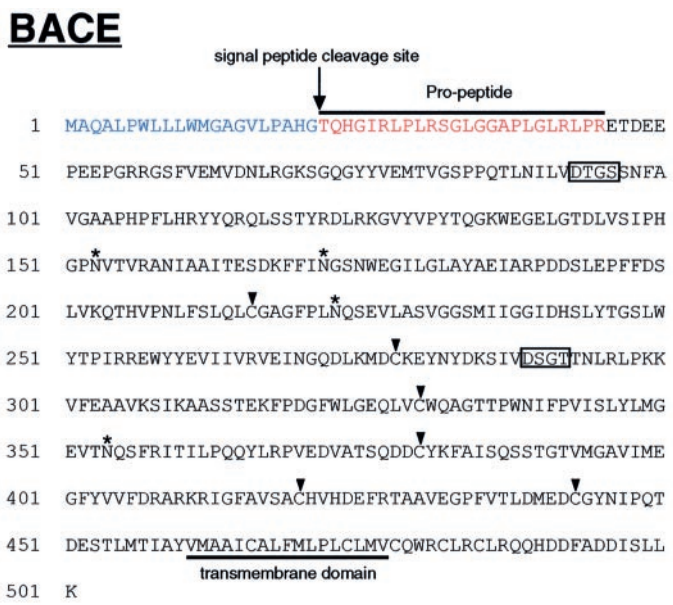

Fig. 2. The deduced amino acid sequence (*38*) of human BACE (GenBank accession number AF190725). Numbers on the left indicate amino acid position; boxes, conserved aspartic protease active site domains; asterisks, predicted N-linked glycosylation sites; arrowheads, lumenal cysteine residues.

chemistry with antibody against the COOH-terminal neoepitope of the β-cleaved APPs (APPsβsw) reveals that APPsβsw generation is dramatically increased in cells overexpressing BACE-HA (Fig. 4B). Moreover, APPsβsw immunostaining largely overlaps with BACE-HA signal, indicating that BACE-HA induces β-secretase cleavage within shared intracellular compartments.

Overexpression of BACE causes increased β-secretase activity. To quantitate the effects of BACE overexpression on APP metabolites, we transiently transfected BACE or vector alone into 293 cells stably expressing either wild-type APP695 (APP wt) or APPsw and measured changes in secreted APP metabolites with enzyme-linked immunosorbent assays (ELISA) for $Aβ_{1-x}$, $Aβ_{x-42}$, APPsα, and APPsβsw (*30*). In both cell types, BACE overexpression did not affect APP expression, as demonstrated by unchanged levels of cellular full-length APP (*24*). In APPwt cells, BACE transfection results in an approximate twofold increase in Aβ production, and this increase is found for both $Aβ_{1-x}$ and $Aβ_{x-42}$, indicating that BACE does not enhance 40 or 42 cleavage specifically (Fig. 5A). In contrast, APPsα is significantly decreased upon BACE transfection (Fig. 5C), suggesting that the Aβ increase is not a result of increased APP expression or turnover but rather is a consequence of a specific increase in the β-secretase cleavage pathway.

To visualize the Aβ-like peptides secreted from the APPwt cells, we immunoprecipitated conditioned media from metabolically labeled BACE- or vector-transfected cells with monoclonal antibody 4G8, which recognizes residues 17 to 24 of Aβ (Fig. 5B). The intensity of the Aβ band is significantly increased upon BACE transfection (left lane) compared to vector transfection (right lane), whereas the α-secretase pathway derived p3 band is almost absent. Instead, a shortened Aβ species appears only slightly above the p3 position, which we identify as the Glu11 product (see below).

Consistent with the results obtained from the APPwt cells, BACE overexpression in APPsw cells caused an approximate twofold increase in production of APPsβsw with a concomitant decrease in APPsα (Fig. 5, E and F). Surprisingly, $Aβ_{1-x}$ and $Aβ_{x-42}$ levels did not change significantly (Fig. 5D), suggesting that BACE overexpression in APPsw cells enhances β-secretase cleavage; however, most of the additional C99 is not converted to Aβ. To determine if there was an intracellular accumulation of C99, we immunoprecipitated cell lysates with an APP COOH-terminal–specific polyclonal antibody (Fig. 5G). A fragment corresponding in size to C99 was three times more abundant in BACE transfected cells (left lane) than in cells transfected with vector alone (right lane). Another fragment running just above C83 was also significantly increased. This fragment, which runs at an estimated size of C89, is consistent with a Glu11 cleavage product (see below). Quantitation of C83 demonstrates a reduction to 70% of the control levels upon BACE transfection (*24*).

Thus, transient overexpression of BACE does not affect APP expression, but it decreases α-secretase cleavage and increases β-secretase activity in cells expressing wt or Swedish mutant APP. Enhanced β-secretase activity is readily detected by increases in the immediate β-secretase cleavage products APPsβsw and C99 in APPsw cells and by increases in Aβ production in the APPwt cells.

BACE overexpression causes cleavage of APP exactly and only at known β-secretase sites. To determine the exact site or sites of BACE-induced cleavage, we radiosequenced Aβ and APP COOH-terminal fragments after metabolic labeling of the cells with ^{3}H-Phe (*8, 22*). We first analyzed the Aβ band (Fig. 5B) of the APPwt cells that had been transfected with vector alone. These cells secrete Aβ, starting predominantly at Asp1 (circles and broken line,

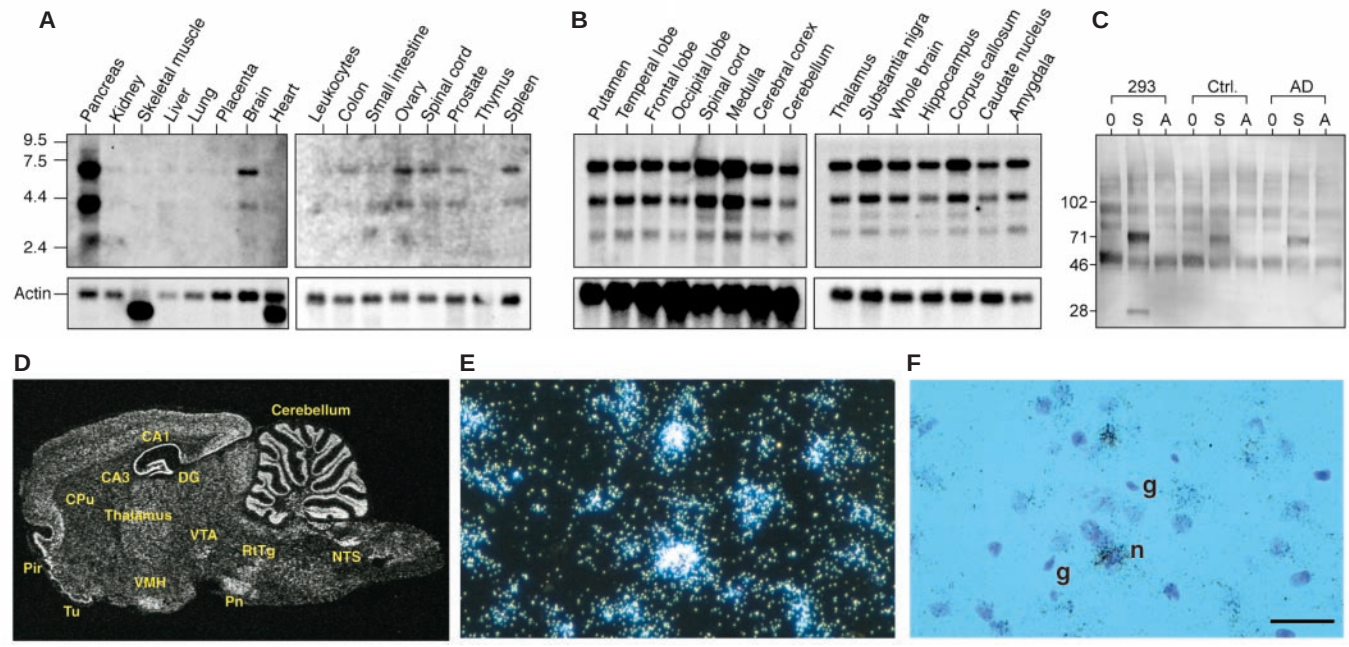

Fig. 3. BACE mRNA and protein expression in peripheral tissues and brain. (**A**) Upper panels: human adult multiple tissue Northern blots (Clontech) hybridized with human BACE cDNA probe (nucleotides −132 to +640). Lower panels: blots were stripped and rehybridized with β-actin cDNA probe as a control. Numbers on the left correspond to molecular size markers (in kilobases). (**B**) Human adult brain sub-region Northern blots hybridized with BACE and β-actin cDNA probes as in (A). (**C**) Immunoprecipitation-immunoblot showing BACE protein expression in Alzheimer's (AD) and control (Ctrl.) brain, and in BACE-transfected cells (293). 0: preimmune serum; S: BACE antiserum; A: BACE antiserum preabsorbed with immunogenic peptide. Numbers on the left correspond to molecular size markers (kD). [(D) to (F)] In situ hybridizations of adult rat brain sections with rat BACE antisense RNA probe (nucleotides +815 to +1593). (**D**) Low magnification image of a parasagital brain section. Abbreviations: CPu, caudate putamen; DG, dentate gyrus; NTS, nucleus of the solitary tract; Pir, piriform cortex; Pn, pontine nuclei; RtTg, reticulotegmental nuclei; Tu, olfactory tubercle; VMH, ventromedial hypothalamic nucleus; VTA, ventral tegmental area. (**E** and **F**) Corresponding high magnification dark-field (E) and bright-field (F) micrographs of cortex. Hybridization signal is observed over most neuronal cell bodies (n), while small, darkly stained glial cells (g) are negative. Bar, 25 μm.

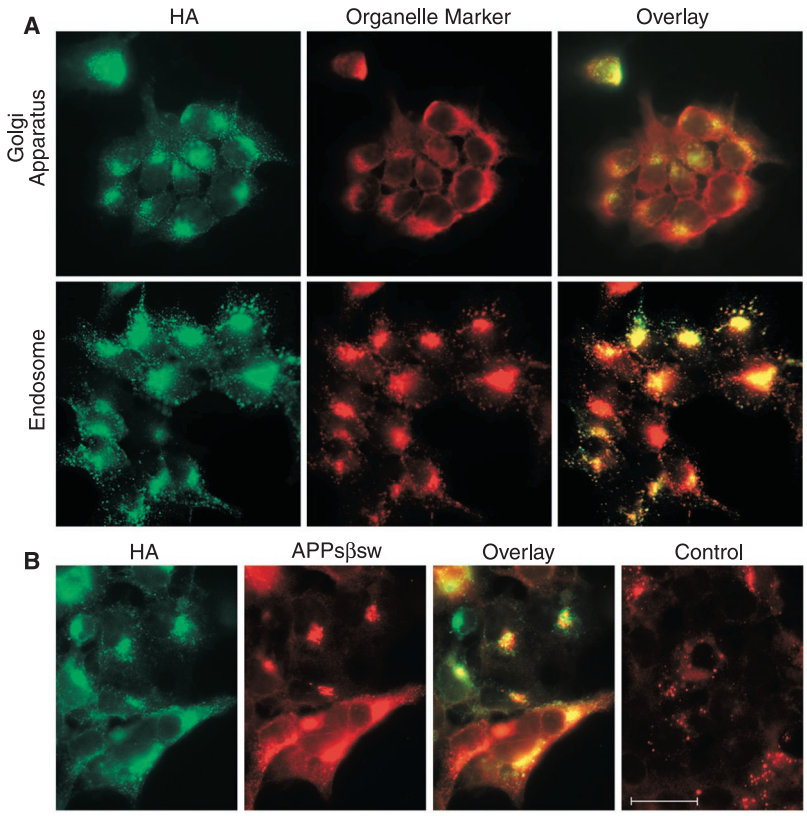

Fig. 4. Intracellular localization of BACE-HA. (**A**) Cells overexpressing BACE-HA were co-stained with antibodies against HA and organelle markers, and observed by fluorescence microscopy. Left: anti-HA immunostaining (green). Middle: anti-organelle marker immunostaining (red). Right: overlay of HA and organelle marker immunostaining. Co-localization of anti-HA and anti-organelle staining appears yellow. Organelle markers: Golgi apparatus, Golgi 58K protein; endosome, transferrin receptor. (**B**) BACE-HA expressing stable cells were transiently transfected with APPsw and costained with antibodies against HA (green) and the APPsβsw neoepitope generated upon β-secretase cleavage of APPsw (red). The overlay shows co-localization of BACE-HA and APPsβsw neoepitope in shared intracellular compartments (yellow). Control cells transfected with APPsw show only limited vesicular staining for the APPsβsw neoepitope, as described in (*12*) (red; control). Bar, 25μm.

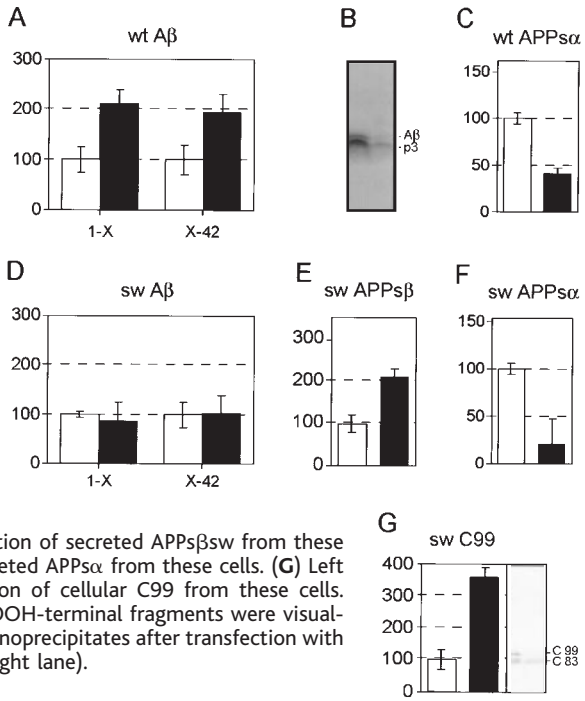

Fig. 5. Effect of BACE overexpression on APP processing in transiently transfected cells. All quantitations are means ± SD of at least four different determinations. The value of the vector-transfected control (white bar) is set at 100%; BACE transfection: black bar. (**A**) ELISA quantitation of secreted $A\beta_{1-x}$ and $A\beta_{x-42}$ from 293 cells expressing APPwt after transfection with BACE. (**B**) total Aβ from these cells was visualized by gel electrophoresis of immunoprecipitates after transfection with BACE (left lane) or vector alone (right lane). (**C**) ELISA quantitation of secreted APPsα from these cells. (**D**) ELISA quantitation of secreted $A\beta_{1-x}$ and $A\beta_{x-42}$ from 293 cells expressing APPsw after transfection with BACE. (**E**) ELISA quantitation of secreted APPsβsw from these cells. (**F**) ELISA quantitation of secreted APPsα from these cells. (**G**) Left panel: phosphorimaging quantitation of cellular C99 from these cells. Right panel: C99 and other APP COOH-terminal fragments were visualized by gel electrophoresis of immunoprecipitates after transfection with BACE (left lane) or vector alone (right lane).

2175 cpm peak in cycle 4) (Fig. 6A); however, minor cleavage products at Val-3 and Ile-6 are also detected, confirming previous results (*8*). Aβ production is enhanced in cells transfected with BACE, and radiosequencing of the Aβ band demonstrates a start exclusively at Asp1 (triangles, 7280 cpm peak in cycle 4; Fig. 6A). The minor species Val-3 and Ile-6 are unchanged and no additional peaks are observed.

To exactly identify the immediate products of β-secretase cleavage, we also radiosequenced the APP COOH-terminal fragments that are enhanced upon BACE transfection into APPsw cells. We first isolated the 12-kD swC99 band, which is nearly indetectable in cells transfected with vector alone (Fig. 5G). As expected, this BACE-induced band starts at Asp1 only (Fig. 6B), demonstrating that BACE overexpression promotes the generation of C99, the precursor of Asp1-Aβ. However, BACE also induces another band migrating just above C83 (Fig. 5G). Because this band could not be excised from the blot separately from C83, we excised it together with C83 and sequenced the same molecular weight range of the sample transfected with vector alone, which contains only C83, as a control (Fig. 6C). Both the vector-transfected and the BACE-transfected cells produce C83 starting at the previously established α-secretase cleavage sites (*31*). However, the strongest signal induced by BACE is at Glu11 (peak at cycles 9, 10) and derives from the band migrating just above C83. This indicates that BACE overexpression promotes Glu11 cleavage and the appearance of C89, the precursor for Glu11-Aβ. In summary, overexpression of BACE induces cleavage only at the known β-secretase positions, Asp1 and Glu11.

Inhibition of β-secretase activity with BACE antisense oligonucleotides. To establish that BACE is required for β-secretase cleavage, we inhibited expression of the endogenous BACE gene by delivering antisense oligonucleotides (AS oligos) into 101 cells by lipid-mediated transfection (*32*). We used three BACE-specific AS oligos (AS#2, AS#3, AS#4) and a reverse sequence oligo as a negative control for each (REV#2, REV#3, REV#4). As additional controls, we generated AS oligos with two, four, or six mismatches (2MIS, 4MIS, 6MIS) distributed within the AS#2 sequence.

We first determined the potency of BACE AS oligo inhibition of endogenous BACE mRNA expression in APPsw cells. In Northern blots hybridized with BACE cDNA probe, the intensity of all three BACE transcripts is dramatically reduced by treatment with AS oligos as compared to reverse sequence oligos, whereas control messages are not affected (Fig. 7A). The AS oligos reduce normalized BACE mRNA levels to only ~25 to 30% of control oligos (Fig. 7B). Treatment with the 2MIS oligo reduces BACE mRNA to an intermediate

level (~45%) between that of AS#2 and REV#2. 4MIS and 6MIS oligos have no effect on BACE mRNA.

Treatment of APPsw cells with AS oligos typically reduced APPsβsw levels to 30 to 40% of that found in cells treated with reverse sequence oligos (Fig. 7C). 2MIS oligo reduces the APPsβsw level to ~70%, a value intermediate between that of AS#2 and REV#2. As expected, 4MIS and 6MIS oligos do not reduce APPsβsw levels. Thus, BACE antisense treatment decreases both BACE mRNA and APPsβsw in parallel and achieves a maximum inhibition of ~75 to 80% for both parameters.

Because α- and β-secretase appear to compete for the same intracellular pool of APP, we predicted that inhibition of β-secretase activity would elevate α-secretase cleavage. Indeed, APPsα levels were increased by 30 to 50% upon BACE inhibition with AS oligos (Fig. 7D), providing further evidence that antisense inhibition is specific for BACE and does not simply decrease APP expression.

Finally, we determined the effect of BACE inhibition on Aβ production in APPsw cells. Typically, AS oligos reduce Aβx-40 and Aβx-42 levels to ~60 to 70% of the levels observed in control oligo treated cells (Fig. 7, E and F). 2MIS oligo has an intermediate inhibitory effect on Aβx-40 and Aβx-42 relative to AS#2 and REV#2, while 4MIS and 6MIS oligos have no effect. The inhibition of Aβ production with BACE AS oligos is significant and reproducible, although it is less than that observed for APPsβsw. However, APPsβsw is an immediate product of Asp1 β-secretase cleavage, while the Aβ assays are not specific for the Asp1 product and depend on γ-secretase cleavage.

Together, these results strongly suggest that BACE is required for β-secretase cleavage and that no other proteases can efficiently compensate for loss of BACE function.

Purified BACE cleaves APP substrates and exhibits the properties of β-secretase. To demonstrate that BACE has β-secretase activity, we developed an in vitro system in which purified BACE directly cleaves peptide substrates containing the appropriate APP sequences. We engineered a soluble BACE–immunoglobulin G (BACE-IgG) fusion protein containing the entire lumenal domain of BACE (amino acids 1–460), fused to the human IgG1 at the COOH-terminus. BACE-IgG was overexpressed in 293T cells and purified from conditioned media (Fig. 8A) (*33*).

To address the substrate requirements of BACE-IgG, we designed three peptide substrates, each containing 30 amino acids, extending from P21 to P9' to span the β-secretase cleavage site. These peptides represent: (i) APPwt; (ii) APPsw; and (iii) the MV substitution (P1 changed from Met → Val). In intact cells, endogenous β-secretase cleaves APPsw much better than APPwt, but the MV mutant is not cleaved (*22*). Pure BACE-IgG cleaves the pure wt peptide with a specific activity of approximately 9 nmol/min/mg, demonstrating that BACE acts as a protease (Fig. 8B). We detect only one cleavage and this is at the correct Asp1 site (*24*). As expected for β-secretase, the specific activity of BACE-IgG for the Swedish substrate is much higher than for the wt substrate, whereas cleavage of the MV mutant is not detectable at all (Fig. 8B).

Experiments with intact cells suggest that β-secretase has an acidic pH optimum (*14, 15*). Indeed, a pH titration of BACE activity shows an optimum at pH 4.5 for both the wt and the Swedish mutant peptide (Fig. 8C). Previous experiments with intact cells did not provide any hints that β-secretase is an aspartic protease. In particular, pepstatin treatment appears to affect γ- but not β-secretase cleavage (*34*). We therefore tested the effect of pepstatin on BACE activity in vitro. Interestingly, BACE is not inhibited by pepstatin even at 30 μM, the highest concentration tested (*24*).

Conclusions. Although the molecular identity of the β-secretase has remained elusive, much has been determined about the characteristics of β-secretase activity in intact cells. We have shown step-by-step that BACE matches all known properties of β-secretase. Its expression pattern and subcellular localization are as expected for β-secretase. Most interestingly, BACE is expressed at higher levels in neurons than in glia. This result supports the idea that neurons are the primary source of the extracellular Aβ deposited in amyloid plaques (*10*). The predicted membrane topology of BACE aspartic protease places the active site within the lumen, in correct topological orientation relative to the β-secretase cleavage site in APP (Fig. 1). Thus, there is no need to invoke unusual mechanisms to explain how the enzyme gains access to its substrate. BACE has an acidic pH optimum and localizes within intracellular compartments of the secretory pathway, in particular Golgi and endosomes, and BACE overexpression induces β-secretase cleavage in these compartments. These characteristics of BACE are consistent with the finding that β-secretase activity is found in acidic subcellular compartments only.

BACE overexpression in cells results in increased β-secretase cleavage of both wild-type APP and Swedish APP. This leads to increased secretion of Aβ peptides from the wt, but not the Swedish mutant cells, which show increased levels of APPsβsw and C99. The reason for this difference is not known, but it is possible that in the APPsw-overexpressing cells, γ-secretase cannot turn over the very high levels of C99. We found decreased levels of αAPPs in conditioned media and of C83 in cell lysates upon BACE overexpression, consistent with the hypothesis that the α- and β-secretase pathways compete for the intracellular APP substrate. The apparently more pronounced reduction of αAPPs compared to C83 may be due to the different detection assays.

Aβ produced in intact cells contains multiple NH_2-termini. The major species starts at

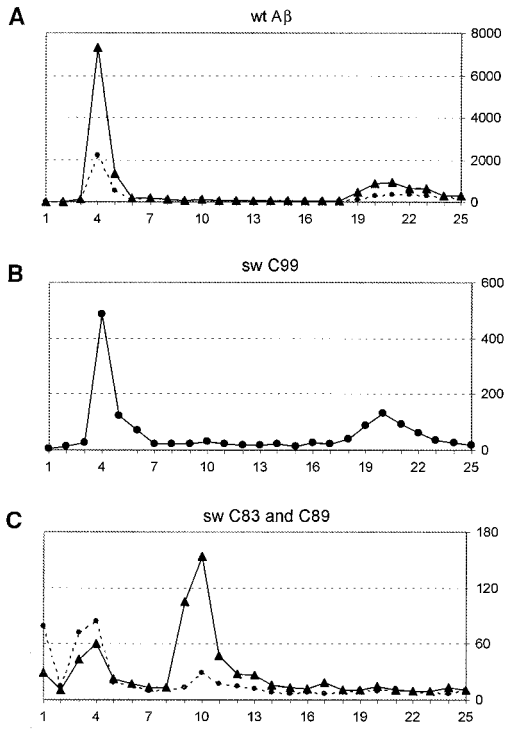

Fig. 6. Radiosequencing of BACE-induced APP metabolites. The figures show radioactivity in counts per min (cpm) per sequencing cycle. (**A**) Sequencing of Aβ from APPwt expressing cells transfected with BACE (triangles) or vector alone (circles and broken line) shows major peaks of ^{3}H-Phe in cycle 4, consistent with Aβ starting at Asp1. This cleavage is increased by BACE transfection. When the scale is expanded, secondary signals at cycles 7 and 10 indicative of Val-3 and Ile-6 cleavage are observed in the vector-alone transfectants (152 cpm and 97 cpm, respectively), but these signals are not increased upon BACE transfection (150 cpm and 110 cpm, respectively). (**B**) Sequencing of the 12 kD band from APPsw expressing cells that is induced upon BACE transfection (Fig. 5G) is consistent with an Asp1 start, indicating that this fragment is indeed C99, the immediate precursor of Asp1-Aβ. (**C**) Sequencing of the C83 and C89 COOH-terminal fragments from APPsw-expressing cells transfected with BACE (triangles) or vector alone (circles and broken line). Vector-alone transfectants show major peaks at cycles 1, 3, and 4, as expected for the previously reported Leu17 and Phe20 start sites of the α-secretase product. BACE transfectants also show these C83 peaks, but the massively enhanced 11-kD band leads to strong signals in cycles 9 and 10, indicating a Glu11 cleavage product.

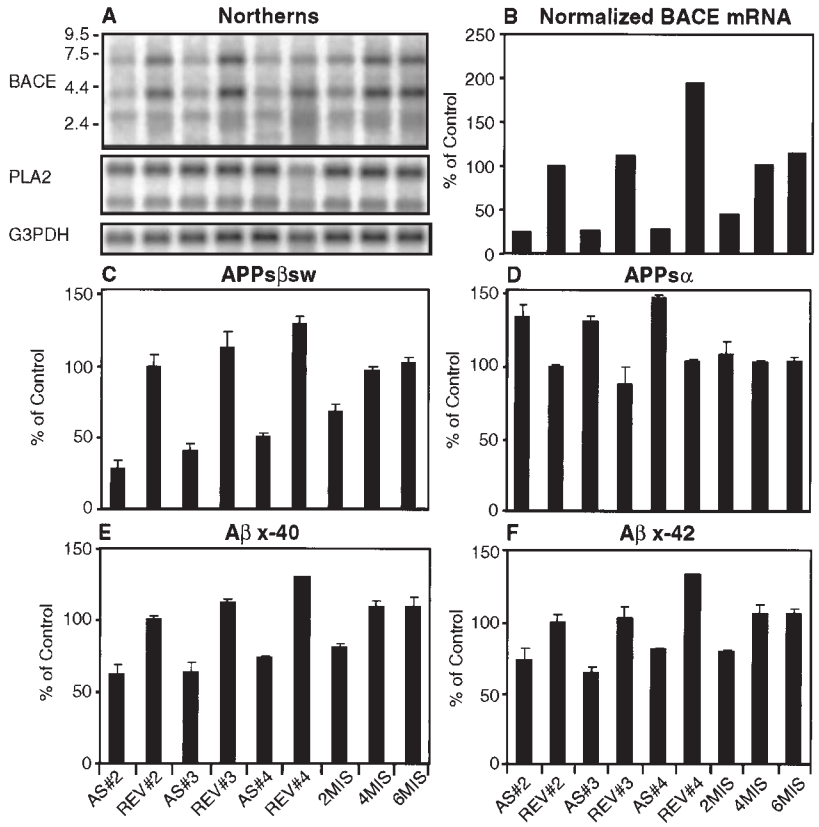

Fig. 7. Antisense inhibition of endogenous BACE in APPsw cells. Cells were treated continuously with AS or control oligos for 48 hours. Media were then collected for ELISA measurements and cells were harvested for RNA isolation. Lane order is indicated at the bottom of (E) and (F), and is the same for all panels. (**A**) Northern blot of poly(A)$^+$ RNA isolated from AS- or control oligo–treated cells and hybridized with BACE cDNA probe (top panel). For normalization, the Nothern blot was stripped and reprobed for phospholipase A2 mRNA (PLA2; middle panel) and glyceraldehyde-3 phosphate dehydrogenase mRNA (G3PDH; bottom panel). Numbers on the left correspond to molecular size markers (in kilobases). (**B**) BACE mRNA counts (4.0 kb transcript) from the Northern in (A) were quantitated by phosphorimaging and normalized to PLA2 mRNA counts (4.0 kb transcript). REV#2 is set at 100%. Note that the REV#4 sample had some RNA degradation, which skewed normalized REV#4 RNA counts to a higher value in comparison to the other controls. [(C) to (F)] ELISA measurements of APPsβsw (**C**), APPsα (**D**), Aβx-40 (**E**), and Aβx-42 (**F**) from conditioned media of AS or control oligo treated cells. Values are the average of triplicate samples ±SD. REV#2 values are set at 100%.

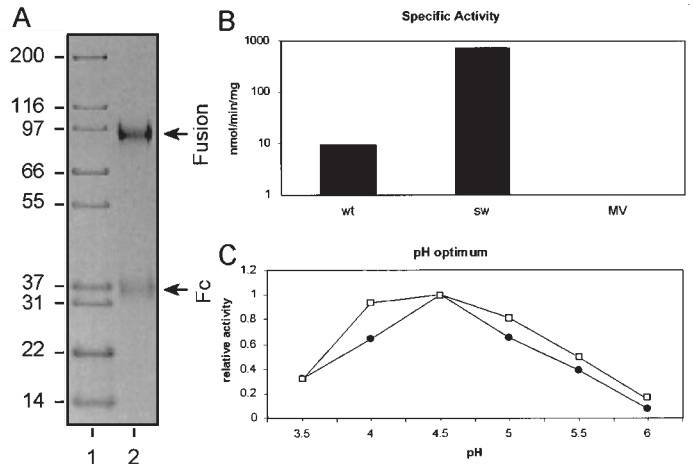

Fig. 8. Purified BACE-IgG cleaves APP-derived substrates. (**A**) silver-stained gel of purified BACE-IgG. Only the fusion protein and some clipped Fc are detected in this enzymatically pure preparation. The enzyme preparation used for the assays did not exhibit any free Fc. Numbers on the left correspond to molecular size markers (kD). (**B**) Specific activity determination of purified BACE-IgG at pH 4.5 on three different substrates. There is no detectable cleavage of the MV mutant substrate. (**C**) The pH dependence of BACE activity. Plotted is the activity (relative to the optimum at pH 4.5 set at 1.0 for each substrate) for wild-type (open squares) and Swedish mutant substrate (black circles).

Asp1, but minor forms starting at Val-3, Ile-6, and Glu-11 have been reported (*8*). In cultured rat neurons, the Glu-11 form appears to be the major Aβ species (*17*). This has raised the question of whether there is one β-secretase or multiple enzymes with different cleavage sites. Inhibitor experiments have suggested that the Asp1 form is modulated differently than the Val-3 and Ile-6 forms (*18, 19*), but in parallel with the Glu11 form (*17*). We find that BACE causes increased APP cleavage at Asp1 and Glu11, but not other positions. We therefore suggest that BACE is the major Asp1 and Glu11 cleaving β-secretase but that other proteases account for the minor Val-3 and Ile-6 forms. Our antisense experiments show that an inhibition of endogenous BACE expression dramatically reduces β-secretase activity, providing direct evidence that BACE not only promotes β-secretase cleavage but is required for this cleavage.

The in vitro experiments with purified BACE-IgG directly demonstrate that BACE has proteolytic activity on APP-derived peptide substrates, excluding the possibility that BACE is simply a cofactor, upstream activator, or facilitator for an unknown β-secretase. Moreover, in these in vitro experiments BACE exhibits the P1 site specificity of β-secretase (*22*). The fact that BACE is pepstatin insensitive explains why β-secretase has not been previously classified as an aspartic protease. A previous study suggested that β-secretase is a serine protease, based on partial inhibition of β-secretase cleavage in intact cells upon treatment with the serine protease inhibitor AEBSF. However, we could not distinguish between direct inhibition of β-secretase and indirect effects attributable to the high AEBSF concentrations used (*18*).

Our data provide strong evidence that the BACE aspartic protease is the long-sought β-secretase. However, ultimate validation must await the analysis of APP-overexpressing transgenic mouse models (for example, *35*) that have been made deficient in BACE by gene targeting.

In future studies, it will be important to investigate whether the expression or processing of BACE is abnormal in Alzheimer's disease and whether BACE alleles exist that increase or decrease the risk of Alzheimer's disease. Finally, the identification of BACE as the major β-secretase may have important medical implications because it will allow application of the standard molecular tools that have led to successful inhibition of other therapeutically relevant aspartic proteases, such as renin and the human immunodeficiency virus I protease.

References and Notes

1. G. G. Glenner and C. W. Wong, *Biochem. Biophys. Res. Commun.* **120**, 885 (1984).
2. S. G. Younkin, *J. Physiol. (Paris)* **92**, 289 (1998).
3. J. Kang *et al.*, *Nature* **325**, 733 (1987).
4. J. D. Buxbaum *et al.*, *J. Biol. Chem.* **273**, 27765

(1998); S. Lammich *et al.*, *Proc. Natl. Acad. Sci. U.S.A.* **96**, 3922 (1999).
5. G. Evin, K. Beyreuther, C. L. Masters, *Amyloid* **1**, 263 (1994).
6. B. De Strooper *et al.*, *Nature* **391**, 387 (1998); B. De Strooper *et al.*, *ibid.* **398**, 518 (1999).
7. M. S. Wolfe *et al.*, *ibid.* **398**, 513 (1999).
8. C. Haass *et al.*, *ibid.* **359**, 322 (1992).
9. P. Seubert *et al.*, *ibid.* **361**, 260 (1993).
10. J. Zhao *et al.*, *J. Biol. Chem.* **271**, 31407 (1996).
11. E. H. Koo and S. Squazzo, *ibid.* **269**, 17386 (1994).
12. C. Haass *et al.*, *Nature Med.* **1**, 1291 (1995).
13. A. S. C. Chyung, B. D. Greenberg, D. G. Cook, R. W. Doms, V. M. Y. Lee, *J. Cell Biol.* **138**, 671 (1997).
14. C. Haass, A. Y. Hung, M. G. Schlossmacher, D. B. Teplow, D. J. Selkoe, *J. Biol. Chem.* **268**, 3021 (1993).
15. J. Knops *et al.*, *ibid.* **270**, 2419 (1995).
16. A. E. Roher *et al.*, *ibid.* **268**, 3072 (1993).
17. G. K. Gouras *et al.*, *J. Neurochem.* **71**, 1920 (1998).
18. M. Citron *et al.*, *Neuron* **17**, 171 (1996).
19. A. Capell, D. B. Teplow, M. Citron, D. J. Selkoe, C. Haass, *Amyloid* **3**, 150 (1996).
20. M. Mullan *et al.*, *Nature Genet.* **1**, 345 (1992).
21. M. Citron *et al.*, *Nature* **360**, 672 (1992); X.-D. Cai, T. E. Golde, G. S. Younkin, *Science* **259**, 514 (1993).
22. M. Citron, D. B. Teplow, D. J. Selkoe, *Neuron* **14**, 661 (1995).
23. S. L. Ross *et al.*, *J. Biol. Chem.* **273**, 15309 (1998).
24. R. Vassar *et al.*, data not shown.
25. N. D. Rawlings and A. J. Barrett, *Methods Enzymol.* **248**, 105 (1995).
26. In situ hybridizations were performed using 10-μm sections through fresh frozen brain tissue obtained from adult Sprague-Dawley rats. Antisense riboprobes labeled with ^{35}S-UTP and ^{35}S-CTP were generated from rat BACE cDNA Bgl II–Kpn I fragment (nucleotides +815 to +1593). Hybridization and wash conditions were as described (*36*).
27. A synthetic peptide corresponding to the COOH-terminal 17 amino acids of BACE was synthesized, conjugated to keyhole limpet hemocyanin (KLH), and used to raise a polyclonal antibody. The antibody and preimmune serum (negative control) were coupled to Protein A Sepharose for use in immunoprecipitation assays. Pieces of parietal cortex of human Alzheimer's disease and control brains obtained from Sun Health Research Institute (Arizona) were homogenized in lysis buffer (*22*), and the homogenate was spun at 20,000*g* for 10 min at 4°C. For each immunoprecipitation about 25 mg wet weight equivalent were used. BACE immunoprecipitation from extracts of 293 cells transiently transfected with BACE were carried out as in (*8*), and the precipitates were subjected to SDS-PAGE followed by immunoblotting with the BACE antiserum as primary antibody.
28. For the generation of the BACE-HA cell line, a BACE-HA fusion construct was made containing the nine–amino acid hemagglutinin epitope (*37*) fused in frame at the BACE COOH-terminus.
29. Immunocytochemistry of paraformaldehyde-fixed Triton X-100 permeabilized cells followed standard protocols (*12*). Primary antibodies and dilutions were the following: anti-HA monoclonal or polyclonal antibodies (Covance) 1:100; anti-58K (Sigma) 1:20; and anti-transferrin receptor (Dako) 1:20; anti-APPsβsw 1:500. Alexa 488 (green) and Alexa 594 (red) secondary antibodies (Molecular Probes) were used at 1:200 dilution.
30. Transfection, metabolic labeling, preparation of total cell lysates, immunoprecipitation, and protein radiosequencing were carried out as in (*8*). For immunoprecipitation of APP and its COOH-terminal fragments, we used a polyclonal antibody that we raised to the last 20 amino acids of the cytoplasmic tail of APP. For immunoprecipitation of Aβ we used the monoclonal antibody 4G8 raised to Aβ17-24 (Senetek). Quantitation of APP metabolites was done using time-resolved fluorescence sandwich ELISA assays with unmodified capture antibody and a biotinylated reporter antibody. Europium-labeled streptavidin was then reacted with the biotinylated antibody and the europium was quantitated by Delfia time-resolved fluorescence. For quantitation of total Aβ ($Aβ_{1-x}$), we established an ELISA using monoclonal antibody 4G8 as capture and biotinylated monoclonal antibody 6E10 raised to Aβ1-17 (Senetek) as reporter. This assay detects all forms of Aβ with an intact NH_2-terminus. For quantitation of all Aβ derivatives ending at amino acid 42 ($Aβ_{x-42}$), we established an ELISA using anti-Aβ 42, a purified rabbit polyclonal antibody that specifically recognizes the 42 form of Aβ (Biosource International) as capture and biotinylated 4G8 as reporter. This assay detects all forms of Aβ and p3 that end at amino acid 42. A similar ELISA for detection of $Aβ_{x-40}$ was established using anti-Aβ 40, a purified rabbit polyclonal antibody which specifically recognizes the 40 form of Aβ (Biosource International). For quantitation of APPsα we used a polyclonal antibody raised to the APP midregion (total APP) as capture and biotinylated 6E10 as reporter. For quantitation of APPsβsw, we raised a polyclonal antibody specific for the β-secretase generated neoepitope of APPsw and used this antibody as capture, followed by biotinylated monoclonal antibody 5A3 (total APP) (*11*) as reporter.
31. Z. Zhong *et al.*, *J. Biol. Chem.* **269**, 627 (1994).
32. Antisense oligonucleotides complementary to BACE mRNA were generated (Sequitur): AS#2 (5′-GUCCUGAACUCAUCGUGCACAUGGC-3′); AS#3 (5′-CAUCUGUGUCUCCUACUUGUGACCA-3′); and AS#4 (5′-CCAAGAGUAUUCCCGCCAGCAGAGU-3′). A reverse sequence control oligonucleotide for each antisense oligonucleotide was also synthesized. The following AS#2 mismatch control oligonucleotides were made: 2MIS (5′-GUCCUGAAGUCAUCGUCCACAUGGC-3′); 4MIS (5′-GUCCAGAAGUCAUCGUCCACUUGGC-3′); and 6MIS (5′-GGCCAGAAGUCAUCGUCCACUUGUC-3′). The APPsw cells were plated in 6-well dishes at 396,000 cells/well. After reaching ~70 to 80% confluency, cells were treated in triplicate with antisense or control oligonucleotide continuously for 48 hours in the presence of serum using a lipid delivery system (Sequitur). Cells were then washed and fresh medium was added for 6 to 8 hours of conditioning. Conditioned media were collected and assayed by APPsβsw, APPsα, Aβx-40, and Aβx-42 ELISAs. In addition, cells from triplicate wells were harvested and pooled for isolation of polyadenylated [poly(A)$^+$] RNA (Micro-FastTrack; Invitrogen). Northern analysis was performed as described above. For normalization, blots were stripped and reprobed with phospholipase A2 and glyceraldehyde-3 phosphate dehydrogenase cDNA probes (Clonetech; Palo Alto, CA). Blots were visualized and quantitated using a Storm 860 phosphoImager (Molecular Dynamics).
33. For the soluble BACE-IgG cell line, we generated a fusion construct encoding BACE amino acids 1–460 (ending at the start of the predicted transmembrane sequence) fused in frame with a three–amino acid linker (alanine-valine-threonine) and the Fc portion of human IgG1 (starting at amino acid 29; GenBank accession number X70421). BACE-IgG was purified from conditioned media of stably transfected 293T cells with Protein A columns. Substrate peptides were synthesized and labeled with dinitrophenol at P8′ to allow easy ultraviolet detection of cleavage products after reversed phase high performance liquid chromatography. The APPwt substrate sequence was TTRPGSGLTNIKTEEISEVKMDAEFRHDK(dnp)G; in the Swedish mutant variant, KM is substituted by NL, and in the MV mutant, M is substituted by V. All assays were performed with the same batch of BACE-IgG. Substrates were used at 30 μM in a 50-μl assay. All assays were buffered with 50 mM acetic acid (pH 4.5) unless otherwise indicated. Enzyme and substrate were incubated between 30 min and 18 hours at room temperature, then the reaction mixtures were quenched and analyzed by reversed-phase HPLC. Both product and substrate were monitored by absorbance at 360 nm. Products were identified by retention time comparison with a reference peptide run under identical conditions.
34. M. P. Murphy *et al.*, *J. Biol. Chem.* **274**, 11914 (1999).
35. D. Games *et al.*, *Nature* **373**, 523 (1995).
36. E. J. Curran and S. J. Watson, *J. Comp. Neurol.* **361**, 57 (1995).
37. J. Field *et al.*, *Mol. Cell Biol.* **8**, 2159 (1988).
38. Single-letter abbreviations for the amino acid residues are as follows: A, Ala; C, Cys; D, Asp; E, Glu; F, Phe; G, Gly; H, His; I, Ile; K, Lys; L, Leu; M, Met; N, Asn; P, Pro; Q, Gln; R, Arg; S, Ser; T, Thr; V, Val; W, Trp; and Y, Tyr. X indicates any residue.
39. We thank E. H. Koo for monoclonal antibody 5A3, T. Woolf for technical advice on antisense experiments, G. Zajic for help with microscopy, and N. Davidson, T. Livelli, and J. Ngai for helpful discussions. We also thank D. Paulin, D. Olivares, and G. Zajic for preparation of figures.

10 September 1999; accepted 27 September 1999

Contact-Dependent Inhibition of Cortical Neurite Growth Mediated by Notch Signaling

Nenad Šestan,[1] Spyros Artavanis-Tsakonas,[2] Pasko Rakic[1]*

The exuberant growth of neurites during development becomes markedly reduced as cortical neurons mature. In vitro studies of neurons from mouse cerebral cortex revealed that contact-mediated Notch signaling regulates the capacity of neurons to extend and elaborate neurites. Up-regulation of Notch activity was concomitant with an increase in the number of interneuronal contacts and cessation of neurite growth. In neurons with low Notch activity, which readily extend neurites, up-regulation of Notch activity either inhibited extension or caused retraction of neurites. Conversely, in more mature neurons that had ceased their growth after establishing numerous connections and displayed high Notch activity, inhibition of Notch signaling promoted neurite extension. Thus, the formation of neuronal contacts results in activation of Notch receptors, leading to restriction of neuronal growth and a subsequent arrest in maturity.

Cerebral cortical neurons grow by extending neurites (that is, axons and dendrites) and forming connections until they reach a mature size, at which their capacity to grow and remodel their connections becomes markedly reduced (*1*). The molecular mechanisms that regulate